CrossMark

Vortex Reconnections in Anisotropic Trapped Three-Dimensional Bose–Einstein Condensates

T. Wells · A. U. J. Lode · V. S. Bagnato · M. C. Tsatsos

Abstract Quantum vortex reconnections can be considered as a fundamental unit of interaction in complex turbulent quantum gases. Understanding the dynamics of single vortex reconnections as elementary events is an essential precursor to the explanation of the emergent properties of turbulent quantum gases. It is thought that a lone pair of quantum vortex lines will inevitably interact given a sufficiently long time. This paper investigates aspects of reconnections of quantum vortex pairs imprinted in a Bose–Einstein condensate with 101 bosons held in an anisotropic three-dimensional trap using an exact many-body treatment. In particular, the impact of the interaction strength and the trap anisotropy in the reconnection time is studied. It is found that interaction strength has no effect on reconnection time over short time scales and that the trap anisotropy can cause the edge of the condensate to interfere with the reconnection process. It is also found that the initially coherent system fragments very slowly, even for a relatively large interaction strength, and therefore the system tends to stay condensed during the reconnections.

T. Wells
Department of Applied Mathematics and Theoretical Physics, University of Cambridge,
Cambridge CB3 0WA, UK
e-mail: tjw78@cam.ac.uk

T. Wells · V. S. Bagnato · M. C. Tsatsos (✉)
Instituto de Física de São Carlos, Universidade de São Paulo, CP 369, São Carlos,
SP 13560-970, Brazil
e-mail: marios@ifsc.usp.br

V. S. Bagnato
e-mail: vander@ifsc.usp.br

A. U. J. Lode
Department of Physics, University of Basel, Klingelbergstrasse 82, 4056 Basel, Switzerland
e-mail: axel.lode@unibas.ch

1 Introduction

Bose–Einstein condensation was first predicted theoretically in 1924 by Bose and Einstein for noninteracting bosonic particles. Its first experimental realization was only achieved in 1995 in interacting dilute atomic vapors, by Anderson et al. [1] and independently by Bradley et al. [2] and Davis et al. [3]. This peculiar finding has since sparked significant research interest in ultracold bosonic gases and their dynamics. Among the numerous unique features of Bose–Einstein condensates (BECs) are the superfluid properties. Specifically, the nucleation and interaction of quantized vortices and turbulent behavior are of exceptional interest. Quantized vorticity follows from the single-valuedness of the superfluid wavefunction and plays a crucial role in the dynamics of the BECs [4]. An understanding of quantum turbulence, i.e., the chaotic interaction of numerous quantum vortex lines, has long been sought and remains an active area of research [5–9].

Quantum vortices were first observed experimentally in BECs in 1999–2000 [10–12]. Decades earlier, the Gross–Pitaevskii equation (GPE) had been devised in order to describe vortices in superfluids [13–16]. A vortex reconnection is a general phenomenon in which two vortex lines interact and exchange tails. In 1987 Ashurst and Meiron simulated the reconnections with a Biot–Savart model [17] and later on, in 1993, Koplik and Levine showed that quantum vortex reconnections appear in the dynamics of the GPE [18]. In 1994 Waele and Aarts with a Biot–Savart model claimed the existence of a universal route to reconnection for all kinds of initial vortex–antivortex arrangements [19]. More recent relevant work includes the study of vortex reconnections in untrapped superfluids [20], in trapped BECs at finite temperatures [21], the computation of the minimum distance between two approaching vortices [22], and the calculation of the energy spectra of gases with reconnecting vortices [23,24]. Despite similarities in the vortex dynamics across various quantum systems, the results on quantum turbulence obtained for a BEC cannot be automatically applied to the theory of turbulence in other quantum fluids (see Ref. [6] for a detailed discussion).

Contemporary approaches to quantum turbulence focus on drawing classical analogies and contrasting them with the quantum case. This can be considered a top-down approach to understanding turbulent dynamics, using what is already known about classical dynamics to understand quantum dynamics. Today the GPE is the foremost basis for the study of quantum turbulence. Yet, as a mean-field theory it neglects crucial quantum effects such as fragmentation and system correlations or even the angular symmetries of the isotropic gas [25]. An alternative approach to understand quantum turbulence is to treat the problem in the true quantum many-body context; study at first the dynamics of simple vortex configurations and extrapolate then to systems containing more vortices. This approach constitutes a bottom-up approach to the problem, putting the quantum dynamics at the heart of the picture. The present paper treats the problem of understanding vortex dynamics with this second approach.

The vast majority of previous studies of the three-dimensional vortex dynamics has been carried out in uniform systems. Experiments with trapped gases however necessitate simulations of vortex interactions in non-homogeneous systems. In the present work, we solve the time-dependent many-body Schrödinger equation as an initial value problem in three dimensions, for a state of the trapped gas containing two perpendicular vortices. This initial state can be created by various vortex imprint techniques (see for instance Ref. [26]). The many-body method used to solve the time-dependent Schrödinger equation is the Multi-Configurational Time-Dependent Hartree for Bosons (MCTDHB) [27–29] and its recursive software implementation (R-MCTDHB) [30]. This method allows us to study the dynamical fragmentation of the system and look for beyond mean-field phenomena. We study the dynamics of the vortices for different values of the interaction strength and of the trap anisotropy. Both parameters are of experimental relevance and expected to impact the dynamical evolution of the system and, more specifically, the time for the quantum vortex reconnection. It is found that the quantum vortex reconnection can follow two separate paths, depending on the anisotropy of the confinement: either through tail exchange between the two vortices in the region of high density (isotropic or close to isotropic trap) or at the border of the cloud, in regions of low density (strongly anisotropic trap). The former is the standard route to quantum vortex reconnection (see for instance Ref. [5]) and we call it herein 'X-reconnection'. The latter is—to the best of our knowledge—unseen before and we term it 'Z-reconnection' due to the peculiar shape of the topology of the quantum vortex reconnections. A sketch of these distinct reconnection paths is shown in Fig. 1.
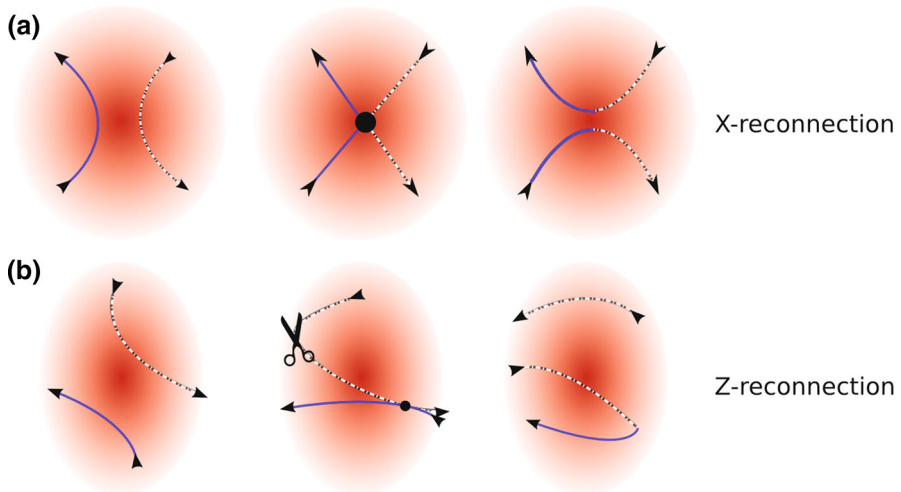

Fig. 1 Schematic depiction of two distinct topologies of the reconnection of the quantum vortices. *Row* **a** shows the *X*-reconnection of the two vortices in a symmetric trap (the vortex lines reconnect in an X-shaped topology). The reconnection always happens in regions of higher density, i.e., at the center of the trap. *Row* **b** shows the Z-reconnection in a gas that is asymmetrically confined ($\omega_y/\omega_x \gtrsim 3/2$ and the vortex lines follow a Z-shaped topology). The reconnection in **b** does not occur at a single point as in **a**; the cut of the reconnection happens near the boundary where the scissors are shown and the paste between the two vortices occurs at the *black dot* which is also near the boundary, but on the opposite side (Color figure online)

The structure of the paper is the following. Section 2 introduces the system Hamiltonian and defines the quantities of interest that will be used. It outlines the vortex imprinting method that defines the initial state of the system. Section 3 presents the results of the calculations and in Sect. 4 conclusions are drawn.

2 System Hamiltonian and Initial State

We study a system of $N = 101$ dilute bosons at zero absolute temperature $T = 0$ that are trapped in a harmonic potential in three spatial dimensions. We solve the time-dependent many-body Schrödinger equation as an initial value problem where the initial state is fixed to posses two perpendicular vortex lines and evolve this state by propagating in real time. The time-dependent Schrödinger equation reads

$$i \frac{\partial}{\partial t} \Psi = \hat{H} \Psi, \tag{1}$$

where the Hamiltonian is

$$\hat{H}(\mathbf{r}_1, \mathbf{r}_2, ..., \mathbf{r}_N) = \sum_{i=1}^{N} \hat{h}(\mathbf{r}_i) + \lambda_0 \sum_{i<j}^{N} \hat{W}(\mathbf{r}_i - \mathbf{r}_j). \tag{2}$$

Here $\mathbf{r}_i$ is the position of the ith boson, λ_0 is the interaction strength, and $\hat{W}$ is the interaction potential. The one-body Hamiltonian operator is $\hat{h}(\mathbf{r}_i) = -\frac{1}{2}\hat{\nabla}^2_{\mathbf{r}_i} + \hat{V}(\mathbf{r}_i)$ with

$$\hat{V}(\mathbf{r}_i) = \frac{1}{2}\omega_x^2 x_i{}^2 + \frac{1}{2}\omega_y^2 y_i{}^2 + \frac{1}{2}\omega_z^2 z_i{}^2, \tag{3}$$

the operator corresponding to the confining trap. Our trap is characterized by the anisotropy on the $x-y$ plane which is quantified by the axis ratio (or anisotropy parameter):

$$\varepsilon = \frac{\omega_y}{\omega_x},$$

while ω_z is kept fixed at unity. The interparticle interaction potential $\hat{W}$ is a Dirac delta, $\delta(\mathbf{r} - \mathbf{r}')$, representing a contact interaction. Equation 2 is dimensionless and can be made dimensionful by multiplying by the unit of energy $\frac{\hbar^2}{mL^2}$.[1]

The MCTDHB method assumes a general many-body ansatz for the solution of the time-dependent Schrödinger equation which is an expansion over a set of many-body basis functions, also known as permanents [27–29]. Each of the permanents describes a condensed or fragmented system and is time dependent. MCTDHB is a theory that solves the many-body Schrödinger equation using an approximation that systematically goes beyond the Gross-Pitaevskii (GP) ansatz. It can be interpreted as a set of M different but mutually interacting superfluids that can exchange particles. In

---

[1] L is chosen to be $L = 1\,\mu\text{m}$, m is taken to be the mass of an ^{87}Rb atom, $m = 86.90918u$ [31], such that the scaling factor corresponds to an angular frequency of $\omega = 731\,\text{rad/s}$.

the case of $M = 1$ it boils down to the GP equation and hence contains it as a limiting simplest case. In our case we choose $M = 2$ orbitals and the expansion becomes:

$$|\Psi\rangle = \sum_{k=0}^{N} C_k(t)|N-k, k; t\rangle. \tag{4}$$

The permanents $|N-k, k; t\rangle$ are built over the two orbitals ϕ_1, ϕ_2 and, together with the coefficients $C_k(t)$, are determined variationally at each time t. Note that the $k = 0$ contribution in the above ansatz, $|N, 0; t\rangle$, is the GP ansatz. The MCTDHB ansatz therefore contains the GP ansatz as the special case of $C_0(t) = 1$ in Eq. 4. A guess wavefunction is relaxed into the ground state Ψ_{gnd} by propagating in imaginary time until the energy is converged. From Ψ_{gnd} the orbitals $\phi_{1,\text{gnd}}$, $\phi_{2,\text{gnd}}$ are obtained. Their occupations are found to be close to 100 and 0 %, respectively. The initial state of two orthogonal vortices is constructed by defining a new wavefunction Ψ using a modified ϕ_1:

$$\phi_1(\mathbf{r}; t=0) = \mathcal{N} \phi_{1,\text{gnd}} \left[\tanh\left(\sqrt{\left(\frac{z-z_0}{\sigma_z(z)}\right)^2 + \left(\frac{y}{\sigma_y(y)}\right)^2} \right) \exp\left(i \tan^{-1}\left(\frac{y}{z-z_0}\right) \right) \right.$$

$$\left. + \tanh\left(\sqrt{\left(\frac{z+z_0}{\sigma_z(z)}\right)^2 + \left(\frac{x}{\sigma_x(x)}\right)^2} \right) \exp\left(i \tan^{-1}\left(\frac{x}{z+z_0}\right) \right) \right]. \tag{5}$$

$\mathcal{N}$ is a renormalization constant. The above state possesses one vortex parallel to the x-axis passing through $(0, 0, +z_0)$ and a second vortex parallel to the y-axis passing through $(0, 0, -z_0)$ at $t = 0$. The parameters $\sigma_x(x) = \sigma_{x0}e^{x^2/4}$, $\sigma_y(y) = \sigma_{y0}e^{y^2/4}$, $\sigma_z(z) = \sigma_{z0}e^{z^2/4}$ define the width of the vortex core. $\sigma_{x0}, \sigma_{y0}, \sigma_{z0}$ are found, such that the energy $\langle\Psi|\hat{H}|\Psi\rangle$ is minimal. The values that we found and used for the different anisotropies are shown in Table 1. The exponential modulation follows from the fact that the size of the vortex core at equilibrium is of the order of magnitude of the healing length ξ. Since the latter is inversely proportional to the square root of the density of the gas, the vortex core is so too. For the interaction strength chosen, the cloud density profile is well approximated by a Gaussian shape so the vortices are expected to 'open out' as we move towards the edge of the gas. The tanh functional form of the initial state of Eq. 5 was chosen such that the density vanishes along the lines ($z = z_0, y = 0$) and ($z = -z_0, x = 0$) while the complex exponential terms create phase profiles that have quantized circulation about the vortex cores. It is important to note, that the vortex imprinting solely in the first orbital ϕ_1 is sufficient in order to create the vortex pair in the many-body wavefunction: since in the ground state Ψ_{gnd} of the parabolic potential the first orbital occupation is larger than 99.9 %, the wavefunction is almost fully determined by the orbital ϕ_1 on which the vortices are imprinted.

Herein we choose $z_0 = 0.5$. The energy of the two-vortex state (Eq. 5) as compared to the ground state with no vortices is found to increase by a factor of approximately 2, for all choices of the interaction strength. Thus, energetically, our ansatz seems not

Table 1 Values of the optimized vortex core parameters $\sigma_{x_0}, \sigma_{y_0}, \sigma_{z_0}$ (optimal values where the energy is minimized for $z_0 = 0.5$) for $g = \lambda_0(N-1) = 10$ and different anisotropies

ε	1–1.4	1.5–1.9	2–2.9	3
$\sigma_{x_0}, \sigma_{y_0}, \sigma_{z_0}$	10,10,10	10,12,10	10,15,10	10,16,10

For the isotropic cases $\varepsilon = 1.0$ and $g = 0.1, 1, 100$ the values $\sigma_{x_0} = \sigma_{y_0} = \sigma_{z_0} = 10$ were used. Precisely, for $\varepsilon = 1$, the energy is minimized by infinitely large $\sigma_{x_0}, \sigma_{y_0}, \sigma_{z_0}$. However, we use a cut-off at {10, 10, 10}; beyond these values the energy drops marginally and the shape of the imprinted vortex does not change visibly

to be a major disturbance to the ground state. The above initial state is propagated in real time and the quantities of interest are calculated. In what follows, we define the density, occupation numbers, and reconnection time.

The one-body reduced density matrix is defined as

$$\rho^{(1)}(\mathbf{r}|\mathbf{r}'; t) = N \int \mathbf{dr}_2 ... \mathbf{dr}_N \Psi^*(\mathbf{r}', \mathbf{r}_2, ..., \mathbf{r}_N; t) \Psi(\mathbf{r}, \mathbf{r}_2, ..., \mathbf{r}_N; t), \qquad (6)$$

which can be decomposed into its eigenfunctions

$$\rho^{(1)}(\mathbf{r}|\mathbf{r}'; t) = N \sum_{i=0}^{M} \rho_i^{(NO)}(t) \phi_i^*(\mathbf{r}'; t) \phi_i(\mathbf{r}; t), \qquad (7)$$

where $\rho_i^{(NO)}(t)$ are the natural occupations and $\phi_i(t)$ the natural orbitals. A many-body system is said to be condensed when $\rho_k^{(NO)} \sim N$ for some k, i.e., when only one natural orbital is macroscopically occupied [32]. When multiple occupation numbers $\rho_i^{(NO)}$ are of the order of N then the system is called fragmented [33]. The *density* in real space is defined as the diagonal of the reduced density matrix $\rho(\mathbf{r}, t) = \rho^{(1)}(\mathbf{r}|\mathbf{r}' = \mathbf{r}; t)$. The numerically calculated density is a four-dimensional array and in order to visualize it we plot isosurfaces of constant ρ at given time steps (see Figs. 2 and 3) and compile them into videos [36]. The numerical analysis is done with a discrete variable representation on a grid of 128^3 grid points, extending from -8 to $+8$ in each spatial dimension.

3 Results

As descriptive quantities for the dynamics of the quantum vortex reconnection, we use the *reconnection begin time* and *reconnection end time*. These are defined as the first moment at which the density isocontours connect and disconnect, respectively. An error bar with magnitude of the time resolution (between 0.10 and 0.25) is ascribed to each data point, indicating that the densities were calculated at this time step. For example, in the simulation shown in Fig. 2 we find a vortex reconnection begin time of $t = 0.70 \pm 0.10$ and a vortex reconnection end time of $t = 2.70 \pm 0.10$.

Variation of the interaction strength Dimensional analysis of the GPE reveals that one can define a "healing time" τ, in direct analogy to the healing length ξ of the condensate as

ε=1.0, g=10   X-reconnection

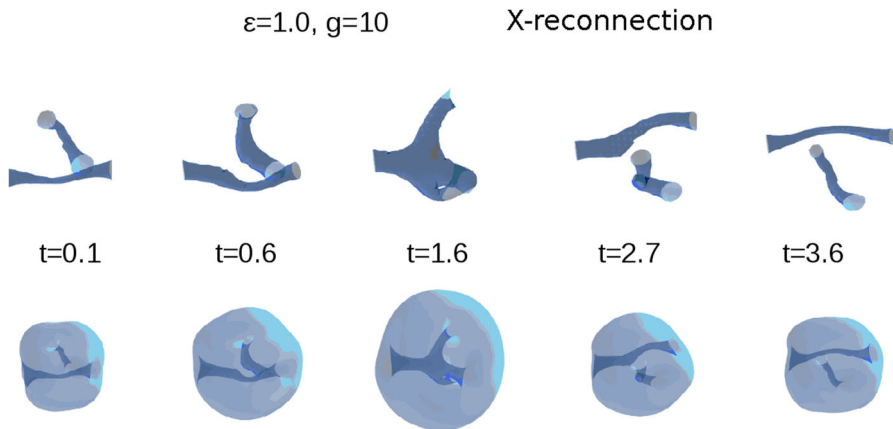t=0.1   t=0.6   t=1.6   t=2.7   t=3.6

Fig. 2 Quantum vortex X-reconnections for $\varepsilon = 1$. Plots of the real-time dynamics for the symmetric trap, at different times. The *top row* of the figures is zoomed in to the bulk density and the *bottom row* shows the whole grid, plotted with an opacity of 0.25. The isosurface values for each time point are defined by the minimum value of the density plus 0.05 times the peak-to-peak (i.e., maximum minus minimum) value of the density. The vortices reconnect at the center of the trap where the density is maximal. The reconnection induces remarkable bulk density oscillations. The occupation numbers of the orbitals however remain almost unchanged. Video simulations of the dynamics for longer times are available [36] (Color figure online)
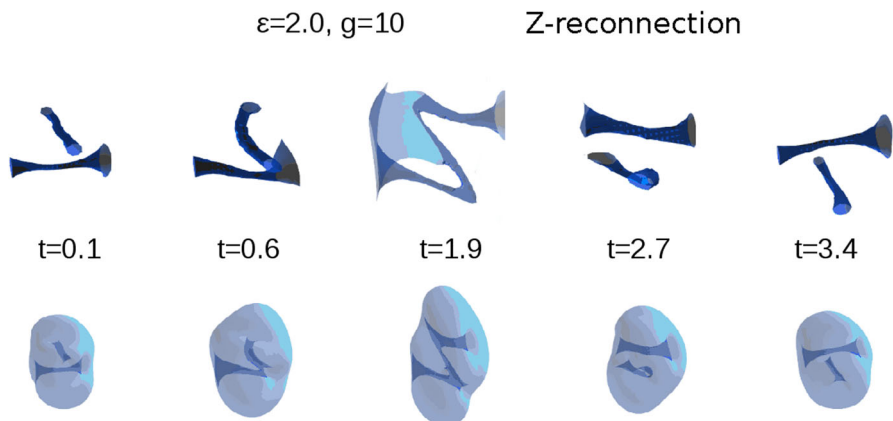
ε=2.0, g=10   Z-reconnection

t=0.1   t=0.6   t=1.9   t=2.7   t=3.4

Fig. 3 Quantum vortex Z-reconnections for $\varepsilon = 2$. Plots of the real-time dynamics for the asymmetric trap, at different times. The vortices reconnect towards the edge of the trap where the density is minimal. As in the previous case, remarkable bulk density oscillations are seen in phase with the reconnections. The occupation numbers of the orbitals however remain almost unchanged and close to 100 and 0 % for the first and second natural orbitals, respectively, throughout the reconnection. Video simulations of the dynamics for longer times are available [36] (Color figure online)

$$\tau = \frac{m\xi^2}{\hbar} = \frac{m}{\hbar g\rho_0},$$

where ρ_0 is a representative constant value of the unperturbed density [34]. In words, this is the time that it takes for the condensate to heal a perturbation over ξ. Hence, for increasing interparticle interaction $g = \lambda_0(N-1)$, the healing time of a perturbation

Table 2 Vortex reconnection times for a scan over $g = \lambda_0(N-1)$ values and fixed $\varepsilon = 1$

g	Reconnection begin time	Reconnection end time
0.1	0.60	3.0
1	0.60	3.0
5	0.65	3.0
20	0.65	3.0
50	0.60	3.0
100	0.60	3.0

These results show that the dynamics of the first reconnection are marginally changed for a range of g values, from weak to moderately strong, over three orders of magnitudes. The error on each time data point is ± 0.05

decreases. This simple analysis suggests a scaling in time with g; the dynamics in systems that interact more strongly happen faster. This motivates the investigation of the role of the interaction strength, g, in the vortex dynamics and also of how the time evolution of fragmentation of the system will be affected.

In Fig. 2 an example reconnection can be seen. We plot the densities, as found from the solution of the time-dependent Schrödinger equation in real time, for the case $\varepsilon = 1$, $g = \lambda_0(N-1) = 10$ at different times: before, during, and after the reconnection. A standard X-reconnection is seen: the two vortices approach each other and they reconnect close to the center of the trap by exchanging tails.

Keeping the anisotropy fixed at $\varepsilon = 1$ (spherically symmetric trap) we now study the quantum vortex reconnection for the values $g \in \{0.1, 1, 5, 10, 20, 50, 100\}$ of the interaction parameter. Repeating the study of the quantum vortex reconnection for all these values of g, we calculate the reconnection begin and end times for each case. Interestingly, we saw that the interaction strength plays no significant role in the vortex reconnection begin/end time for our choice of initial state (see Table 2). Even though the total spatial expansion of the density is, as expected, larger for larger g the differences in the profile of the vortices as they evolve in time is not noticeable. The dynamics of the quantum vortex reconnection are *not* significantly affected by the changes in the strength of the interparticle interaction, at least for the values of g examined here, that span three orders of magnitude. This is in agreement with Ref. [35] where it is found that the nonlinearity of the GPE plays a minor role in the vortex reconnection.

It was found that, on the timescale of the first reconnection, the system does not fragment even for the larger interaction strength values (maximum $g = 100$). This demonstrates that for the system parameters and initial conditions studied, the time-dependent GPE would be a sufficient model for the time scales presented here. One can thus see that the quantum vortex reconnection has no immediate effect on the orbital occupations. For larger g values ($g = 10$ and $g = 100$), we saw that the system fragments only slowly over time. Indeed, in the case of $\varepsilon = 1.0$ and $g = 10$ we have found that for times as long as $t = 100$, the first natural occupation stays above 90 %. In other words, for the time scale when the first approximately 30 reconnections happen the gas stays close to a condensed state. This echoes the classical hydrodynamic result
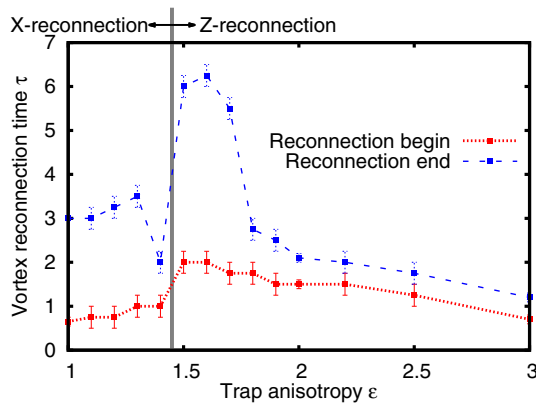
Fig. 4 Quantum vortex reconnection times for varying trap anisotropy parameter ε and g=10. For values up to $\varepsilon = 1.4$ no significant change in the begin/end time are seen as ε increases. The jump in reconnection time from $\varepsilon = 1.4$ to $\varepsilon = 1.5$ is indicative of the change in reconnection type (see *vertical gray line* in the plot), from the *X*-reconnection shown in Fig. 1a to the *Z*-reconnection shown in Fig. 1b in which the quantum vortex reconnection happens toward the edge of the cloud. For larger values of ε the vortices stay connected for shorter times (Color figure online)

that suggests that a significant part of the reconnection process is just the approach of vortex tubes. Though, it could well be that for later times the state cannot be considered condensed anymore and quantum correlations become important and affect the quantum vortex reconnection events.

Interestingly, we have found that, in the isotropic trap, the minimal distance between the vortex lines before the reconnection follows a square root law as a function of time. This is expected and discussed in the context of hydrodynamical models [19]. It is left as future task to determine whether the same law persists in anisotropic traps.

Variation of anisotropy We now turn to the study of the dependence of the quantum vortex reconnection on the trap anisotropy, $\varepsilon = \frac{\omega_y}{\omega_x}$.

For values $1.0 \leq \varepsilon \leq 1.4$ the quantum vortex reconnection happens through a similar mechanism to that of Fig. 2, i.e., it is an *X*-reconnection. However, for $\varepsilon > 1.4$ the quantum vortex reconnection is shifted towards the edge of the condensate. The vortices, due to the anisotropy, tend to align and they follow a different path: they reconnect in regions of low density, i.e., the edge of the cloud instead of the center of the trap. The whole process has a different topology (*Z*-reconnection) than the previously discussed case (*X*-reconnection). Figure 3 shows the *Z*-reconnection of the strongly anisotropic gas. See also Fig. 1, that highlights the difference between the *X*- and *Z*-reconnections. One sees in the central image of this figure a 'Z' shape, which occurs when one of the initial vortices has bent so much that the curved section has met the edge of the condensate bulk. This causes a break in the vortex line and forms one vertex of a 'Z' shape. Simultaneously, one end of the bent vortex meets the end of the other initial vortex to form the second vertex of the 'Z' shape.

We repeated the calculations for various different values of the anisotropy parameter ε and g=10. In Fig. 4 the first quantum vortex reconnection begin and end times are plotted as a function of ε. The change in the path of quantum vortex reconnection,

from X- to Z-reconnection creates a large change in the times associated with the reconnection, which can be seen between $\varepsilon = 1.4$ and $\varepsilon = 1.5$ in Fig. 4. For large trap anisotropies, the Z-reconnection path remains as the reconnection method and the reconnection events happen faster as the edge of the cloud is pushed closer to the position of the initial vortex line.

An interesting common feature that all the simulations share is the bulk oscillations during the quantum vortex reconnection: the cloud expands and reaches a maximum volume at the moment of the quantum vortex reconnection, seemingly *in phase* with the quantum vortex reconnection. Furthermore, calculations for times as long as $t = 140$ suggest that the repeating reconnections persist and occur indefinitely. In Ref. [36], the reader can see videos of the real-time dynamics for the cases of $\varepsilon = 1.0$, 2.0, and 3.0.

4 Conclusions

From the results presented in this work, three main conclusions can be drawn. The first is that there is no direct connection between vortex reconnection and system fragmentation for the coherent initial state containing two orthogonal vortices. We found no significant deviations in the orbital occupations at the short time scales at which the vortex reconnection occurs. For long times, the occupation of the first orbital settles at approximately little less than 90 %. The second conclusion is that reconnection begin and end times are unaffected by variations of the interaction strength. Hence the quantum vortex reconnection dynamics do not appear to scale in time with the interaction. In other words, as the interaction increases and the density at the center decreases the velocities of the vortices in the quantum vortex reconnection do not change. One could ask if the same behavior persists for even larger g and very strongly repulsive gases. The last principal conclusion is that different anisotropies can lead to different routes for reconnection which significantly change the system dynamics. This is shown in Figs. 2 and 3 and in the videos in Ref. [36]. It was also found that the vortex reconnections will occur repeatedly for long times: approximately 40 quantum vortex reconnection happen at a time interval equal to 20 trap periods.

Among a handful of publications that deal with vortex reconnections in trapped BECs, the present paper is the first research into the many-body nature of vortex dynamics and reconnections in three-dimensional trapped ultracold Bose gases. Furthermore it is, to the best of our knowledge, the first work to numerically study quantum vortices in highly asymmetric traps and in a many-body context in three spatial dimensions. As a next step, it would be appealing to study the dynamics of *initially fragmented* vortices and look for many-body mechanisms of vortex reconnection that go beyond the commonly applied Gross–Pitaevskii mean-field method. We hope that the present work will stimulate experimental research.

References

1. M.H. Anderson, J.R. Ensher, M.R. Matthews, C.E. Wieman, E.A. Cornell, Science **269**, 198 (1995)
2. C.C. Bradley, C.A. Sackett, J.J. Tollett, R.G. Hulet, Phys. Rev. Lett. **75**, 1687 (1995)
3. K.B. Davis, M.-O. Mewes, M.R. Andrews, N.J. van Druten, D.S. Durfee, D.M. Kurn, W. Ketterle, Phys. Rev. Lett. **75**, 3969 (1995)
4. R.P. Feynman, Prog. Low Temp. Phys. **1**, 17 (1955)
5. W.F. Vinen, J.J. Niemela, J. Low Temp. Phys. **128**, 167 (2002)
6. S.K. Nemirovskii, Phys. Rep. **524**, 85 (2013)
7. E.A.L. Henn, J.A. Seman, G. Roati, K.M.F. Magalhães, V.S. Bagnato, Phys. Rev. Lett. **103**, 045301 (2009)
8. E.A.L. Henn, J.A. Seman, G. Roati, K.M.F. Magalhães, V.S. Bagnato, J. Low Temp. Phys. **158**, 435 (2009)
9. A.C. White, B.P. Anderson, V.S. Bagnato, Proc. Natl. Acad. Sci. USA **111**, 4719 (2014)
10. M.R. Matthews, B.P. Anderson, P.C. Haljan, D.S. Hall, C.E. Wieman, E.A. Cornell, Phys. Rev. Lett. **83**, 2498 (1999)
11. K.W. Madison, F. Chevy, W. Wohlleben, J. Dalibard, Phys. Rev. Lett. **84**, 806 (2000)
12. K.W. Madison, F. Chevy, W. Wohlleben, J. Dalibard, J. Mod. Opt. **47**, 2715 (2000)
13. E.P. Gross, Il Nuovo Cimento **20**, 454 (1961)
14. L.P. Pitaevskii, Soviet Phys.-JETP (USSR) **13**, 451 (1961)
15. A.L. Fetter, Rev. Mod. Phys. **81**, 647 (2009)
16. A.L. Fetter, J. Low Temp. Phys. **161**, 445 (2010)
17. W.T. Ashurst, D.I. Meiron, Phys. Rev. Lett. **58**, 1632 (1987)
18. J. Koplik, H. Levine, Phys. Rev. Lett. **71**, 1375 (1993)
19. A.T.A.M. de Waele, R.G.K.M. Aarts, Phys. Rev. Lett. **72**, 482 (1994)
20. R. Tebbs, A.J. Youd, C.F. Barenghi, J. Low Temp. Phys. **162**, 314 (2010)
21. A.J. Allen, S. Zuccher, M. Caliari, N.P. Proukakis, N.G. Parker, C.F. Barenghi, Phys. Rev. A **90**, 013601 (2014)
22. S. Zuccher, M. Caliari, A.W. Baggaley, C.F. Barenghi, Phys. Fluids **24**, 125108 (2012)
23. S.K. Nemirovskii, J. Low Temp. Phys. **171**, 504 (2013)
24. S.K. Nemirovskii, Phys. Rev. B **90**, 104506 (2014)
25. M.C. Tsatsos, A.I. Streltsov, O.E. Alon, L.S. Cederbaum, Phys. Rev. A **82**, 033613 (2010)
26. R. Zamora-Zamora, M. Lozada-Hidalgo, S.F. Caballero-Benítez, V. Romero-Rochín, Phys. Rev. A **86**, 053624 (2012)
27. A.I. Streltsov, O.E. Alon, L.S. Cederbaum, Phys. Rev. Lett. **99**, 030402 (2007)
28. O.E. Alon, A.I. Streltsov, L.S. Cederbaum, J. Chem. Phys. **127**, 154103 (2007)
29. O.E. Alon, A.I. Streltsov, L.S. Cederbaum, Phys. Rev. A **77**, 033613 (2008)
30. A.U.J. Lode and M.C. Tsatsos, The Recursive Multiconfigurational Time-Dependent Hartree for Bosons Package, version 1.0, (2014), http://ultracold.org
31. J.R. de Laeter, J.K. Böhlke, P. de Biévre, H. Hidaka, H.S. Peiser, K.J.R. Rosman, P.D.P. Taylor, Pure Appl. Chem. **75**, 683 (2003)
32. O. Penrose, L. Onsager, Phys. Rev. **104**, 576 (1956)
33. P. Noziéres, D. Saint, J. Phys. (Paris) **43**, 1133 (1982)
34. V.I. Yukalov, A.N. Novikov, V.S. Bagnato, Laser Phys. Lett. **11**, 095501 (2014)
35. S. Nazarenko, R. West, J. Low Temp. Phys. **132**, 1 (2003)
36. Videos of the reconnections for: $\varepsilon = 1$ http://youtu.be/VLMY1eYLr0g, $\varepsilon = 2$ http://youtu.be/r5pY7pfMTUg, $\varepsilon = 3$ http://youtu.be/ifEFffVv93U